

## IMRT point dose measurements with a diamond detector

Erin Barnett, Marc MacKenzie, B. Gino Fallone

Department of Physics, University of Alberta, and Department of Medical Physics,  
Cross Cancer Institute, Edmonton, Alberta, USA

---

**Background.** Radiation dose distribution calculations used in treatment planning systems (TPS) describe dose deposition well for large fields. For small fields encountered in Intensity Modulated Radiation Therapy (IMRT) these models may be less accurate. Dose verification of IMRT fields is therefore essential in IMRT implementation and quality assurance. For these smaller fields, lateral electronic equilibrium may not exist and volume averaging effects in ion chambers become increasingly problematic. For this reason, detectors with sensitive volumes smaller than that of conventional ion chambers are preferable in both small fields and high dose gradient region. Diamond detectors are capable of making such accurate dosimetric measurements.

**Methods.** This study compares dosimetry measurements made with a PTW-Freiburg type 60003 diamond detector, an Exradin A12 ion chamber, a PTW-Freiburg PinPoint ion chamber and a Varian a5500 EPID. Dose measurements were made in a clinical prostate intensity modulated beam. Due to difficulties encountered when dosimetric measurements are made in high dose gradient regions, probe positioning within IMRT fields was investigated and a method to establish better probe positions is proposed. Measured doses were compared with HELAX-TMS calculated doses to verify performance of the TPS used in this center.

**Results.** The diamond detector dosimetry is extremely sensitive to positioning particularly in high dose gradient regions. The results indicate that improved agreement between doses measured with various dosimeters can be obtained by appropriate selection of the probe position. Avoidance of high dose gradient regions improves agreement between measured doses particularly for the PinPoint chamber, the diamond detector and the EPID.

**Conclusions.** The use of diamond detectors and EPIDs in dosimetry is an attractive option particularly for verification of IMRT treatments. Although 2D dose verification of IMRT treatments is a more desirable option than point dose verification, an independent check of EPID or film verification is beneficial. Use of a diamond detector is an excellent option for dose measurements in cases where portal imaging devices are not available such as the case of helical tomotherapy.

*Key words:* radiotherapy dosage; radiotherapy; diamond detector, intensity modulated radiotherapy

---

Received 4 August 2004  
Accepted 14 August 2004

Correspondence to: Prof. B. Gino Fallone, PhD, FC-CPM, ABMP, Department of Physics and Oncology, University of Alberta, and Department of Medical Physics, Cross Cancer Institute, Edmonton, Alberta; Phone: +1 780 432-8750; Fax: +1 780 432-8615; E-mail: gfallone@phys.ualberta.ca

## Introduction

The present day movement in radiation therapy is towards intensity modulated radiation therapy (IMRT). The aim of these conformal radiation treatments is to achieve a higher dose within the target volume(s) while minimizing the damage to the organs at risk. IMRT improves upon the technique of 3D conformal radiation therapy by not only improving the conformation of the treated volume to the target volume, but by allowing for more homogeneous doses to be delivered to target volumes.<sup>1</sup> IMRT is a particularly valuable technique when target volumes are concavely shaped and closely neighbored by sensitive volumes that can tolerate very little radiation damage.<sup>2</sup> The fields required to deliver intensity modulated treatments in step and shoot IMRT consist of a number of beam segments that can be more complex in shape than fields previously encountered in radiation therapy. Not only are the segments making up individual IMRT fields smaller than conventional radiotherapy beams, but higher dose gradients are also present in intensity modulated beams (IMB). Within high dose gradients volume averaging effects become more pronounced particularly for large volume point dosimeters. Volume averaging of a signal is not a significant problem if the signal is constant or changes in a linear manner within the sensitive volume of the detector.<sup>3</sup> In high dose gradients the response of a detector may differ substantially from the absorbed dose.<sup>4</sup> A reduction in the size of the sensitive volume yields a reduction in the magnitude of volume averaging effects and therefore leads to more accurate measurements in high dose gradient regions. Also within these dose gradients electronic equilibrium may not exist. The effect of electronic disequilibrium on dosimetric measurements in narrow beams has been investigated by various groups, particularly in the field of stereotactic radiosurgery.<sup>6-8</sup> According to Heydarian *et al.*, ion chamber

based dosimetry in steep dose gradients in the absence of lateral electronic equilibrium is not appropriate.<sup>8</sup> The presence of ion chambers in a radiation field enhances the lateral electronic disequilibrium.<sup>9</sup> Bjärngard *et al.* examined the effect of incomplete lateral electronic equilibrium on central axis dose measurements and made comparisons with Monte Carlo simulation. This group concluded that the detector's sensitive volume must be significantly smaller than the radius of the stereotactic beam in which dosimetric measurements are to be made. Their simulations indicated that at a beam radius of 1.5 cm, lateral electronic equilibrium was reached for a 6 MV simulated beam.<sup>5</sup> For higher beam qualities, a larger field size is required to ensure the existence of lateral electronic equilibrium.

Diamond detectors are an attractive option for making dosimetric measurements in small fields due to the inherently small sensitive volume of these devices as well as energy and directional independence as documented by a number of groups.<sup>10-12</sup> In a study conducted by Heydarian *et al.* it was found that lateral electronic disequilibrium can cause dose measurement errors particularly for large volume non-tissue equivalent detectors.<sup>8</sup> Since diamond detectors are small volume essentially tissue equivalent dosimeters, the presence of lateral electronic equilibrium is not a strict requirement for diamond detector dosimetry.

The objective of this investigation was to determine the feasibility of making point dose measurements in IMBs that may contain small segments and high dose gradients. Dose measurements in solid water phantom were conducted for 15 MV linear accelerator generated beam generated by a Varian 2100 EX linear accelerator [Varian Medical Systems, Palo Alto, CA]. Dose measurements were made using a PTW-Freiburg type 60003 diamond detector, Exradin A12 ion chamber, PTW-Freiburg PinPoint ion chamber and a Varian aS500 EPID.

## Materials and methods

The diamond detector employed in this study is a type 60003 (S/N 9-032) [PTW-Freiburg, Germany]. The sensitive volume consists of a natural diamond crystal with a sensitive area of 6.8 mm<sup>2</sup>, a thickness of 0.25 mm giving a sensitive volume of 1.7 mm<sup>3</sup>. This volume is oriented in the probe housing such that the sensitive volume is positioned 1 mm from the front face of the cylindrical probe. Prior to all dosimetric measurements, the diamond detector was irradiated to a dose of at least 5 Gy to ensure the stability of the response.

Diamond detectors are known to exhibit a dose rate dependence that is described by

$$i = R \cdot (\dot{D})^\Delta + i_{\text{dark}} \quad [1]$$

where  $i$  is the diamond current,  $R$  is a constant of proportionality,  $\dot{D}$  is the dose rate,  $\Delta$  is the sublinear response parameter of the diamond detector and  $i_{\text{dark}}$  is the dark current of the detector.<sup>13,14</sup> The magnitude of the dark current of diamond detectors is sufficiently small that this additive term in this equation can be neglected. The  $\Delta$  and  $R$  value of this detector are  $0.995 \pm 0.002$  and  $0.0254 \pm 0.0003$  nA/cGy/min, respectively. Corrections for the dose rate dependence were made according to equation 1.

The PinPoint ion chamber used in this study is a PTW-Freiburg type 31006 (S/N 0290) [PTW-Freiburg, Germany]. This detector has a 0.015 cm<sup>3</sup> air filled sensitive volume. The wall material is 0.56 mm of PMMA and 0.15 mm of graphite. The sensitive volume is cylindrical in shape with a length of 5 mm and a radius of 1 mm. The pre-irradiation dose of 2 Gy as recommended in the instruction manual was delivered prior to all dosimetric measurements.

The primary substandard ion chamber used by this centre is an Exradin A12 ion chamber (S/N 396) [Standard Imaging, Middleton, WI]. This dosimeter is a Farmer type chamber with a collecting volume of

0.651 cm<sup>3</sup>. The diameters of the sensitive volume and the collector are 6.1 mm and 1.0 mm respectively. The wall, collector and guard material of this device are made with Shonka air-equivalent plastic C552 with a wall thickness of 0.5 mm.

The Varian Portalvision aS500 EPID [Varian Medical Systems, Palo Alto, CA] consists of an amorphous silicon solid state flat-panel imaging device. Dosimetry measurements using a PortalVision aS500 EPID [Varian Medical Systems, Palo Alto, CA] were made with a technique involving convolution-type calculations described by B. Warkentin *et al.* and S. Steciw *et al.*<sup>15,16</sup>

### *Dosimetry of clinical prostate intensity modulated beam*

The probes were positioned at isocenter of a Varian 2100 EX linear accelerator [Varian Medical Systems, Palo Alto, CA] at a depth of 10 cm in a solid water phantom [Gammex, Middleton, WI] with their axes of symmetry perpendicular to the beam central axis (CAX). The responses of the dosimeters to a step and shoot clinical prostate plan were monitored as a function of time using a Wellhöfer Dosimetrie System [Scanditronix-Wellhofer, Schwarzenbruck, Germany]. The Wellhöfer system outputs a signal in terms of percent dose. In order to relate this percent dose during the delivery of the irradiations at various field sizes, the percent dose response of the dosimeters in a 10 x 10 cm<sup>2</sup> field was also observed for all point dosimeters. At the time of experimentation the output of the linac was measured with a PR-06C Farmer type chamber [CNMC Company, Nashville, TN] in a 10 x 10 cm<sup>2</sup> field in a constancy device that ensures the uniform probe positioning that is used for routine quality assurance. The percent dose output of the Wellhöfer system was converted to a dose rate by making use of the relationship between the Wellhöfer electrometer response to the 10 x 10 cm<sup>2</sup> radiation

field at a depth of 10 cm and the dosimetry measurements under the same conditions. In addition to monitoring the diamond response using the Wellhöfer system, the diamond current response to a  $10 \times 10 \text{ cm}^2$  irradiation field at a depth of 10 cm was monitored using a Keithley 6514 electrometer [Keithley Instruments, Inc., Cleveland, OH]. This additional step is required when conducting dosimetry using a diamond detector as the diamond current is related to the dose rate by equation 1. The percent dose rate output of the Wellhöfer system was converted to a diamond current by means of this cross calibration. The resulting diamond current was subsequently converted to a dose rate. To arrive at the total dose during the IMB delivery, the dose rates were integrated with time. EPID dose distributions for each field segment were measured according to the method described by B. Warkentin *et al* and S. Steciw *et al*. The method described in these works results in the dose distribution at a depth of 10 cm for an source surface distance of 90 cm.<sup>15,16</sup> The central pixel values of the EPID dose distributions for each segment were extracted and compared with doses measured with the point dosimeters.

Dose calculations of this IMB delivered to a water phantom were made using HELAX-TMS [Nucletron, Veenendaal, The Netherlands]. In addition to the IMB, a  $5 \times 5 \text{ cm}^2$  field centered about a different isocenter was included in the calculation space to allow for the conversion of calculated percent doses to doses. This  $5 \times 5 \text{ cm}^2$  field was positioned sufficiently far from the IMBs so that the scatter contribution from this field to the IMB was negligible.<sup>17</sup> Comparison of the calculated point dose at isocenter was made to the dose measured with the various dosimeters.

#### *Dosimetry of clinical prostate intensity modulated beam at improved detector positions*

Due to the difficulties associated with con-

ducting point dose measurements in high dose gradients, it is desirable to make point dose measurements in low dose gradient regions. In order to establish improved detector positions, Matlab code [Mathworks, Natick, MA] was written that excluded probe positions based on their vicinity to segment edges. For a given segment, possible probe positions were deemed acceptable if the beam edges were distanced 1 cm from the probe position thereby avoiding measurement positions within the penumbral regions of that segment. A probe position map for the IMB was then generated based on the acceptable probe positions for each of the segments comprising the beam according to the respective segment weightings in the IMB. Although probe positions outside the treatment field are considered to be improved detector positions according to segment edge exclusion criteria, these positions were not considered to be improved positions. The dose within the treatment field is the quantity of interest, not the dose delivered via scatter to the surrounding volume. Comparison between measured and calculated doses was made.

## Results

### *Dosimetry of clinical prostate intensity modulated beam*

The beam segments that comprise the prostate step and shoot IMB are shown in Figure 1. The coordinates (0,0) of each segment correspond to isocenter. The results of the dose measurements at isocenter of the clinical prostate IMRT treatment are summarized in Table 1.

By viewing the segment shapes shown in Figure 1 it is apparent that the poorest agreement between the measured doses occurs in cases where segment edges abut the point of measurement. This poor agreement is attributed to volume averaging effects within the

sensitive volumes and errors introduced by probe positioning. Although the extremely small sensitive volume of the diamond detector is desirable for many applications, it makes the positioning of the probe critical. Since the thickness of the sensitive volume of

this diamond detector is 0.25 mm, an uncertainty of  $\pm 0.5$  mm in probe positioning can mean the difference between centering the sensitive volume in the open portion of the beam or in the penumbral region of segments that abut the point of measurement. Thus di-

**Table 1.** Doses measured at isocenter during delivery of 8 segment clinical prostate intensity modulated beam

Segment	Dose (cGy)				
	A12	PinPoint	Diamond detector	EPID	HELAX-TMS
1	25.5 $\pm$ 0.4	29.0 $\pm$ 0.2	10.9 $\pm$ 0.1	19 $\pm$ 4	23.6
2	25.9 $\pm$ 0.4	29.5 $\pm$ 0.2	11.2 $\pm$ 0.1	19 $\pm$ 4	23.8
3	26.1 $\pm$ 0.4	28.2 $\pm$ 0.2	15.2 $\pm$ 0.2	21 $\pm$ 4	21.7
4	40.3 $\pm$ 0.6	40.0 $\pm$ 0.3	40.2 $\pm$ 0.5	39.9 $\pm$ 0.1	39.5
5	36.0 $\pm$ 0.4	35.9 $\pm$ 0.2	36.1 $\pm$ 0.5	35.9 $\pm$ 0.1	35.6
6	34.9 $\pm$ 0.5	38.9 $\pm$ 0.3	40.2 $\pm$ 0.5	39.7 $\pm$ 0.1	40.5
7	9.3 $\pm$ 0.1	10.8 $\pm$ 0.1	7.5 $\pm$ 0.1	10 $\pm$ 2	2.7
8	2.18 $\pm$ 0.03	2.24 $\pm$ 0.01	2.26 $\pm$ 0.01	2.5 $\pm$ 0.1	0.0
Total	200 $\pm$ 1	214.5 $\pm$ 0.5	164 $\pm$ 1	186 $\pm$ 7	187

**Table 2.** Doses measured at improved detector position 1 (-1.3 cm 1.7 cm) during delivery of 8 segment intensity modulated field

Segment	Dose (cGy)				
	A12	PinPoint	Diamond detector	EPID	HELAX-TMS
1	2.58 $\bar{\pm}$ 0.04	1.61 $\bar{\pm}$ 0.02	1.40 $\bar{\pm}$ 0.02	1.7 $\bar{\pm}$ 0.1	1.1
2	2.63 $\bar{\pm}$ 0.04	1.65 $\bar{\pm}$ 0.02	1.47 $\bar{\pm}$ 0.02	1.7 $\bar{\pm}$ 0.1	1.1
3	10.1 $\bar{\pm}$ 0.2	3.23 $\bar{\pm}$ 0.05	2.61 $\bar{\pm}$ 0.04	3.0 $\bar{\pm}$ 0.3	2.6
4	40.6 $\bar{\pm}$ 0.7	41.0 $\bar{\pm}$ 0.6	40.9 $\bar{\pm}$ 0.6	40.2 $\bar{\pm}$ 0.1	39.5
5	36.4 $\bar{\pm}$ 0.7	36.9 $\bar{\pm}$ 0.6	36.5 $\bar{\pm}$ 0.6	36.2 $\bar{\pm}$ 0.1	35.6
6	39.4 $\bar{\pm}$ 0.6	40.6 $\bar{\pm}$ 0.5	40.2 $\bar{\pm}$ 0.5	40.0 $\bar{\pm}$ 0.2	39.9
7	5.0 $\bar{\pm}$ 0.1	4.69 $\bar{\pm}$ 0.05	4.61 $\bar{\pm}$ 0.05	4.5 $\bar{\pm}$ 0.5	1.3
8	3.17 $\bar{\pm}$ 0.04	2.75 $\bar{\pm}$ 0.03	2.72 $\bar{\pm}$ 0.03	2.8 $\bar{\pm}$ 0.2	0.0
Total	140 $\bar{\pm}$ 1	132 $\bar{\pm}$ 1	130 $\bar{\pm}$ 1	130.1 $\bar{\pm}$ 0.7	121.2

**Table 3.** Doses measured at improved detector position 2 (0.7 cm, 3.0 cm) during delivery of 8 segment intensity modulated field

Segment	Dose (cGy)				
	A12	PinPoint	Diamond detector	EPID	HELAX-TMS
1	1.23 $\bar{\pm}$ 0.02	1.15 $\bar{\pm}$ 0.01	1.00 $\bar{\pm}$ 0.01	1.36 $\bar{\pm}$ 0.05	0.2
2	1.26 $\bar{\pm}$ 0.02	1.22 $\bar{\pm}$ 0.01	1.04 $\bar{\pm}$ 0.01	1.35 $\bar{\pm}$ 0.04	1.1
3	1.26 $\bar{\pm}$ 0.02	1.18 $\bar{\pm}$ 0.01	1.00 $\bar{\pm}$ 0.01	1.26 $\bar{\pm}$ 0.04	0.9
4	37.3 $\bar{\pm}$ 0.6	39.7 $\bar{\pm}$ 0.3	39.2 $\bar{\pm}$ 0.5	38.4 $\bar{\pm}$ 0.3	39.2
5	33.8 $\bar{\pm}$ 0.5	36.3 $\bar{\pm}$ 0.2	35.6 $\bar{\pm}$ 0.5	35.0 $\bar{\pm}$ 0.2	35.5
6	38.2 $\bar{\pm}$ 0.6	41.2 $\bar{\pm}$ 0.3	40.4 $\bar{\pm}$ 0.5	39.7 $\bar{\pm}$ 0.3	36.6
7	45.6 $\bar{\pm}$ 0.7	49.9 $\bar{\pm}$ 0.3	49.8 $\bar{\pm}$ 0.7	48.7 $\bar{\pm}$ 0.2	49.6
8	36.9 $\bar{\pm}$ 0.6	44.9 $\bar{\pm}$ 0.3	45.6 $\bar{\pm}$ 0.4	44.9 $\bar{\pm}$ 0.1	46.1
Total	196 $\bar{\pm}$ 1	216 $\bar{\pm}$ 1	214 $\bar{\pm}$ 1	210.8 $\bar{\pm}$ 0.5	209.1

amongst detector dosimetry is extremely sensitive to positioning particularly in high dose gradient regions.

The doses calculated by HELAX-TMS appearing in Table II are included for comparative purposes only. It is not assumed that these values represent the most accurate determination of dose.

*Dosimetry of clinical prostate intensity modulated beam at improved detector positions*

The map used to establish improved detector positions for the clinical IMB is shown in Figure 2. The positions within the treatment

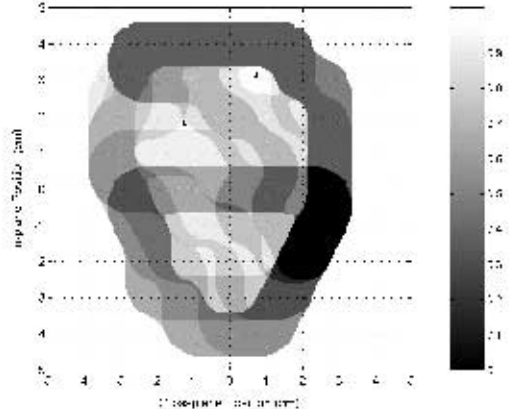


Figure 2. Map used to determine appropriate probe positions for a clinical prostate intensity modulated beam.

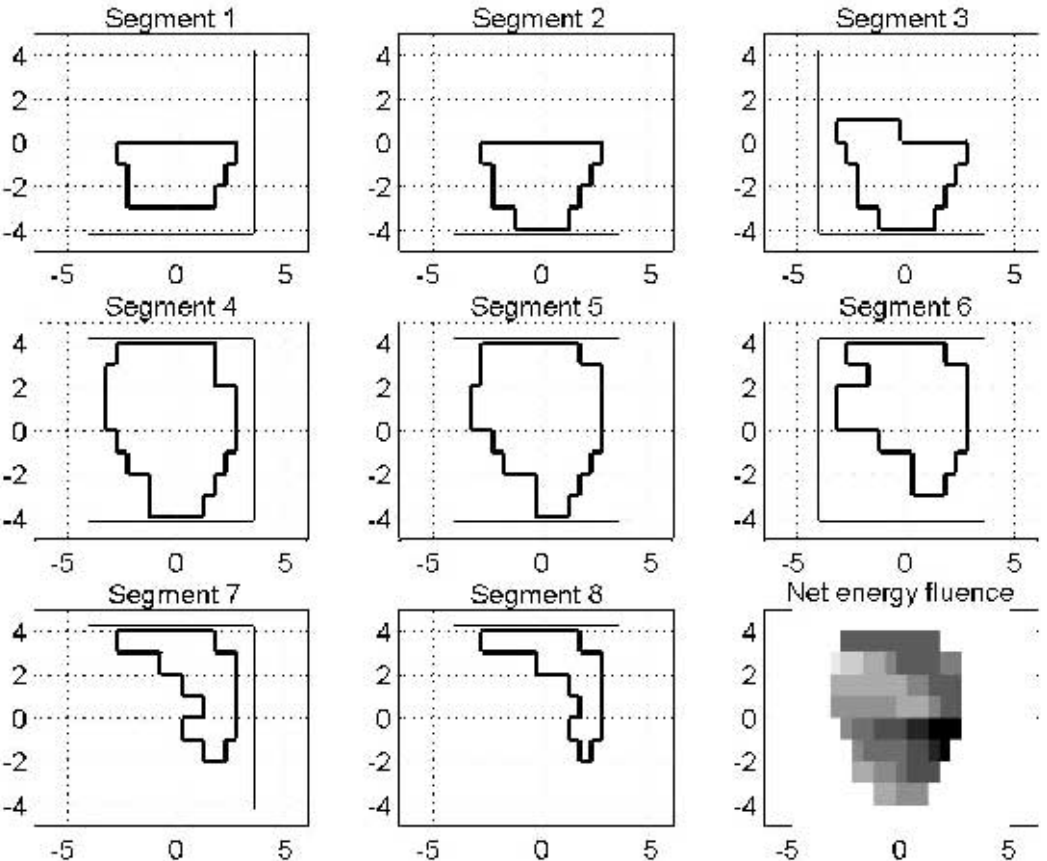


Figure 1. Shape of eight segments that comprise single intensity modulated beam and »fluence map« resulting from delivery of eight step and shoot segments - thick lines illustrate segment geometry, thin lines illustrate main collimator settings.



field with the highest value assigned to them are the most appropriate positions to make point measurements according to the criteria described in the preceding section. The arrows in Figure 2 indicate the positions that best avoid high dose gradients, (0.7 cm, 3.0 cm) and (-1.3 cm, 1.7 cm), the cross-plane and in-plane positions respectively relative to isocenter. The results of the dose measurements at the improved probe positions as established using the in house software of the clinical prostate IMRT treatment are summarized in Tables 2 and 3.

The results summarized in Tables 2 and 3 indicate that improved agreement between doses measured with various dosimeters can be obtained by appropriate selection of the probe position. Avoidance of high dose gradient regions improves agreement between measured doses particularly for the PinPoint chamber, the diamond detector and the EPID. By measuring the dose at the first improved detector position as determined by the technique previously described, excellent results are obtained. The total doses measured by the PinPoint chamber, diamond detector and EPID are very nearly in agreement within one standard error. Although the agreement between the doses measured at the second improved detector position is not as good as at the first improved detector position, the PinPoint and EPID values differ by less than 1.5 % from the diamond detector measured value. Comparison of the results summarized in Tables 1 through 3 indicates that improvement in the agreement between doses measured with various dosimeters can be obtained by choosing measurement points appropriately. Avoidance of high dose gradient regions is necessary to avoid volume averaging effects that greatly affect large volume chamber and to eliminate the high sensitivity of dosimeters to small errors in positioning.

## Discussion

IMRT gives rise to smaller field sizes and higher dose gradients than were previously encountered in conventional radiation therapy with the exception of stereotactic radiosurgery. Point dose measurement of IMBs can be complicated by the presence of high dose gradients within these fields. Dose measurement in the absence of these gradients is necessary to avoid volume averaging effects. The technique employed in this investigation to select better probe positions for the clinical IMB that avoid these high dose gradients gave rise to improved agreement between the dosimeters used in this study. Sub-optimal agreement was obtained between measured and HELAX-TMS calculated doses. This result is attributed to the difficulties associated with penumbral modeling in the release of HELAX-TMS used in this center.

The use of diamond detectors and EPIDs in dosimetry is an attractive option particularly for verification of IMRT treatments. Although 2D dose verification of IMRT treatments is a more desirable option than point dose verification, an independent check of EPID or film verification is beneficial. Use of a diamond detector is an excellent option for dose measurements in cases where portal imaging devices are not available such as the case of helical tomotherapy. Also for accelerators that are equipped with multi-leaf collimators but lack a portal imager, diamond detector dosimetry is a viable technique. The EPID dosimetry technique employed in this study is applicable only to specific geometric conditions at the present time, while diamond detector dosimetry is not limited by these conditions allowing for point verification at different positions and depths within phantom.

## Acknowledgments

E. Barnett would like to thank NSERC and AHFMR for their financial support as well as Dr. S. Steciw and B. Warkentin for use of software to convert EPID images to dose distributions and H. Warkentin for assistance with HELAX-TMS.

## References

1. Martens C, Claeys I, De Wagter C, De Neve W. The value of radiographic film for the characterization of intensity-modulated beams. *Phys Med Biol* 2002; **47**: 2221-34.
2. Webb S. *Intensity-Modulated Radiation Therapy*. Bristol: Institute of Physics Publishing; 2001.
3. Mack A, Scheib SG, Major J, Gianolini S, Pazmandi G, Feist H, et al. Precision dosimetry for narrow photon beams used in radiosurgery-determination of Gamma Knife output factors. *Med Phys* 2002; **29**: 2080-9.
4. Martens C, De Wagter C, De Neve W. The value of the PinPoint ion chamber for characterization of small field segments used in intensity-modulated radiotherapy. *Phys Med Biol* 2000; **45**: 2519-30.
5. Bjarngard BE, Tsai JS, Rice RK. Doses on the central axes of narrow 6-MV x-ray beams. *Med Phys* 1990; **17**: 794-9.
6. Houdek PV, VanBuren JM, Fayos JV. Dosimetry of small radiation fields for 10-MV x rays. *Med Phys* 1983; **10**: 333-6.
7. Arcovito G, Piermattei A, D'Abramo G, Bassi FA. Dose measurements and calculations of small radiation fields for 9-MV x rays. *Med Phys* 1985; **12**: 779-84.
8. Heydarian M, Hoban PW, Beddoe AH. A comparison of dosimetry techniques in stereotactic radiosurgery. *Phys Med Biol* 1996; **41**: 93-110.
9. Heydarian M, Hoban PW, Beddoe AH. Dose rate correction factors for diamond detectors for megavoltage photon beams. *Phys Med Biol* 1997; **13**: 55-60.
10. De Angelis C, Onori S, Pacilio M, Cirrone GA, Cuttone G, Raffaele L, et al. An investigation of the operating characteristics of two PTW diamond detectors in photon and electron beams. *Med Phys* 2002; **29**: 248-54.
11. Laub WU, Kaulich TW, Nusslin F. A diamond detector in the dosimetry of high-energy electron and photon beams. *Phys Med Biol* 1999; **44**: 2183-92.
12. Laub WU, Wong T. The volume effect of detectors in the dosimetry of small fields used in IMRT. *Med Phys* 2003; **30**: 341-7.
13. Laub WU, Kaulich TW, Nusslin F. Energy and dose rate dependence of a diamond detector in the dosimetry of 4-25 MV photon beams. *Med Phys* 1997; **24**: 535-6.
14. Fowler JF, Attix FH. Solid state electrical conductivity doseimeters. In: Attix FH, Roesch WC, editors. *Radiation dosimetry*. Vol. 1. New York: Academic; 1966.
15. Steciw S, Warkentin BM, Rathee S, Fallone BG. A Monte Carlo based method for accurate IMRT verification using the aS500 EPID. *Med Phys* 2003; **30**: 1331.
16. Warkentin B, Steciw S, Rathee S and Fallone B G. Dosimetric IMRT verification with a flat-panel EPID. *Med Phys* 2003; **30**: 3143-55.
17. MacKenzie MA, Lachaine M, Murray B, Fallone BG, Robinson D and Field G C. Dosimetric verification of inverse planned step and shoot multileaf collimator fields from a commercial treatment planning system. *J Appl Clin Med Phys* 2002; **3**: 97-109.